ACS APPLIED BIO MATERIALS

www.acsabm.org

Article

A Synthetic Biosensor for Detecting Putrescine in Beef Samples

Alaa S. Selim, James M. Perry, Mohamed A. Nasr, Jay M. Pimprikar, and Steve C. C. Shih*

Cite This: *ACS Appl. Bio Mater.* 2022, 5, 5487−5496

Read Online

ACCESS | Metrics & More | Article Recommendations | Supporting Information

ABSTRACT: Biogenic amines (BAs) are toxicological risks present in many food products. Putrescine is the most common foodborne BA and is frequently used as a quality control marker. Currently, there is a lack of regulation concerning safe putrescine limits in food as well as outdated food handling practices leading to unnecessary putrescine intake. Conventional methods used to evaluate BAs in food are generally time-consuming and resource-heavy with few options for on-site analysis. In response to this challenge, we have developed a transcription factor-based biosensor for the quantification of putrescine in beef samples. In this work, we use a naturally occurring putrescine responsive repressor-operator pair (PuuR-*puuO*) native to *Escherichia coli*. Moreover, we demonstrate the use of the cell-free putrescine biosensor on a paper-based device that enables rapid low-cost detection of putrescine in beef samples stored at different temperatures. The results presented demonstrate the potential role of using paper-based biosensors for on-site testing, particularly as an index for determining meat product stability and quality.

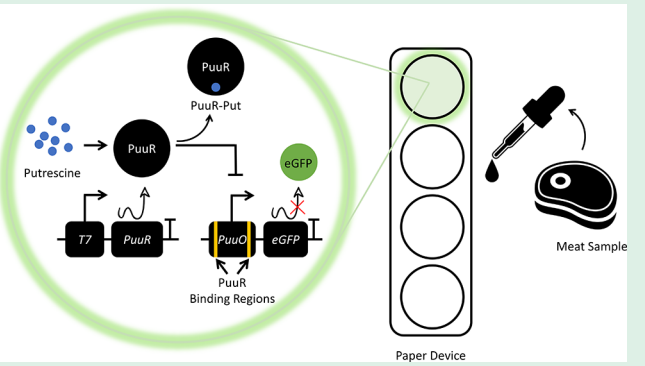

KEYWORDS: *paper-based sensor, biogenic amines, meat spoilage, gene circuit, cell-free transcription-translation, diamines, biosensor*

INTRODUCTION

Quality control of meat products is a major concern for consumer and health agencies because any deviation from proper processing, storage, or distribution may lead to serious biochemical contamination.[1] An example of biochemical contamination is the formation of biogenic amines (BAs), which are typically formed by the microbial decarboxylation of amino acids and are a result of poor hygienic practices.[1] High dietary concentrations of BAs are associated with symptoms including headaches, vomiting, heart palpitations, and diarrhea, and there is an increased risk of developing colorectal carcinoma.[2,3] Putrescine and cadaverine are the two most commonly found BAs in spoiled meats[1] and are used as indicators for meat spoilage in the quality control process.

Strategies for detecting BAs are typically chromatography,[4,5] enzymatic assays,[6] and more recently colorimetric-based assays.[7] Unfortunately, these analytical technologies are not field ready, require specialized equipment to analyze the output, and cannot keep pace with the increased demand for meat products. Additionally, some methods require pretreating food samples with harsh chemicals before analysis, which increases the risk for technicians to develop serious skin allergies, especially if continuous testing is needed.[7] In response to these challenges, transcription factor-based biosensors have been developed for a number of quality control and safety applications. These biosensors have recently demonstrated the detection of a wide range of analytes including amino acids,[8,9] heavy metals,[10] and metabolites[11] and have recently been expanded to include the detection of BAs.[12,13] In some studies, the combination of biosensors with paper-based systems is very attractive for the field since detecting the output uses low-cost detection peripherals[14] or cell-phone cameras,[15] making them ideal for meeting the rising quality control demand.

As far as we are aware, there are only two reports (by Chen et al.[12] and Zhao et al.[13]) that have developed a biosensor for BA detection. These works describe whole-cell biosensors that use cell-based transcriptional circuits to monitor concentrations of putrescine. Our work builds on the work by Chen et al.[12] and Zhao et al.[13] by investigating new synthetic promoters to improve on the limit of detection, dynamic range, sensitivity, and specificity. In addition, we integrated the biosensor with a cell-free expression system[16] to lower the cost and to adapt this platform for use in restaurants, supermarkets, butcher shops and at home. Furthermore, our cell-free BA biosensor is the first to our knowledge that has been applied to consumer beef samples. We propose that our rapid, portable, and user-friendly biosensor platform has the potential to be effectively deployed

Received: September 25, 2022
Accepted: October 27, 2022
Published: November 10, 2022

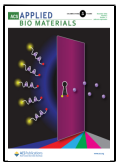

https://doi.org/10.1021/acsabm.2c00824
ACS Appl. Bio Mater. 2022, 5, 5487−5496

in the field, overcoming many of the shortcomings of existing spoilage-detection methods in the food industry.

MATERIALS AND METHODS

Characterization of the Putrescine Biosensor. *Cell Culture and Fluorescence Detection.* In a 96 well plates (Corning Costar 3603, New York, USA), BL21 DE3 star *E. coli* strains were co-transformed with the biosensor plasmids. The biosensor plasmids consisted of a sensing plasmid which expressed the transcription factor PuuR, and a reporter plasmid which expressed eGFP in the presence of putrescine (see Protocol S6 for plasmid construction). Co-transformants were inoculated in 1 mL of M9 minimal media with 50 μg/mL kanamycin and 100 μg/mL carbenicillin and grown overnight in an orbital shaker (Infors-HT, Bottmingen, Switzerland) at 37 °C and 250 rpm. Cultures were diluted 1:100 into 100 μL of fresh M9 minimal media with respective antibiotics and incubated at 37 °C and 250 rpm until the optical density reached 0.3−0.5 (∼3 h). Cultures were induced with 0, 0.1, and 0.5 mM IPTG and supplemented with putrescine to a final concentration of (0, 0.1, 1, 10, 50, 100, 500, and 1000 mM). To create putrescine dilutions, a 2 M stock solution of putrescine (333-93-7, Fisher Scientific) was made by mixing 16.10 g with 50 mL of DNase/RNase free water (Invitrogen) and gently swirled until fully dissolved. Putrescine was pipetted into 500 mL of M9 media to create dilutions of 0, 0.01, 0.1, 1, 10, 100, 1000 mM and mixed with a magnetic stirring bar to ensure homogeneous mixing. The pH was measured with an electronic pH meter and adjusted to 6.5−7.0 using 1 M HCl. Additionally, each plate included the following controls also induced with putrescine: (1) cells without plasmids, (2) cells with only repressor plasmid, and (3) only M9 minimal media. After 16 h, at 37 °C with shaking at 250 rpm, each well was measured for OD_{600} and fluorescence intensity (excitation at 488 nm and emission at 507 nm, gain of 1900) using a well plate reader (CLARIOstar, BMG Labtech, Germany). Fluorescent output was normalized to OD_{600} and background corrected by subtracting the normalized fluorescence of cells lacking the eGFP reporter. All putrescine induction reactions were done in triplicates. All data points were represented as an average with error bars displaying standard error of the mean. Graphs were plotted using GraphPad Prism 9.0, and the fluorescence data was fitted with a Hill function.

Dose−Response and Sensitivity. To plot a dose−response curve, we followed the methodology presented by Mannan et al. and Chen et al.,[12,17,18] which includes parameters such as basal expression ($eGFP_{min}$), maximal expression ($eGFP_{max}$), dynamic range (μ), K_A, and response sensitivity defined as the slope of the dose−response curve or the Hill coefficient "n".

$$y = \mathrm{eGFP}_{\min} + \frac{x^n(\mathrm{eGFP}_{\max} - \mathrm{eGFP}_{\min})}{(x^n + K_A^n)} \quad (1)$$

In eq 1, y represents the normalized fluorescence (RFU/OD_{600}) in accordance with the putrescine concentration at value x. K_A represents the putrescine concentration that induces a response halfway between the baseline and maximum response at a specific putrescine concentration. n is the Hill coefficient which describes the sensitivity, the ability to distinguish small differences in putrescine concentrations.[19,20] $eGFP_{min}$ and $eGFP_{max}$ represent the fluorescence signal from a blank putrescine control with 0.5 mM IPTG and fluorescence signal measured at 16 h, respectively.

Limit of Detection. To calculate the limit of detection (LOD) a linear regression was extrapolated from the dose−response curve for all promoters. From the linear regression, the LOD was calculated using eq 2.

$$\mathrm{LOD} = \frac{3.3(\sigma)}{S} \quad (2)$$

where σ is the standard deviation of the linear range of the dose−response curve and S is the slope of the linear range of the dose−response curve.[21]

Dynamic Range. Dynamic range (μ) was evaluated by measuring the fold change in signal output in the presence and absence of putrescine and was calculated by dividing the normalized fluorescence of $eGFP_{max}$ over $eGFP_{min}$ using eq 3 as a reference.[18]

$$\mu = \frac{\mathrm{eGFP}_{\max}}{\mathrm{eGFP}_{\min}} \quad (3)$$

Specificity. Specificity testing was performed to determine if the biosensor was promiscuous with other analytes. Biogenic amines with very similar molecular structures and characteristics (e.g., histamine and cadaverine) were exogenously added to the whole-cell biosensor (0, 0.1, 1, 10, 50, 100, 500, and 1000 mM), and their output fluorescence was measured following our culture protocol above. To quantify the transcription factor biosensor specificity, we calculated the percent increase of normalized fluorescence in response to cadaverine and histamine compared to putrescine at 50 mM (closest value to our target putrescine concentration).

Time Response. An overnight culture was made the previous day with the appropriate antibiotic selection. Cultures were diluted 1:100 into 100 μL of fresh M9 minimal media with respective antibiotics and incubated at 37 °C and 250 rpm until the optical density reached 0.3−0.5 (∼3 h). Cultures were induced with 0.5 mM IPTG and supplemented with putrescine to a final concentration of 50 mM and pipetted up and down to ensure homogeneous mixing. The 96-well plate was covered with breatheasy seal (Sigma, Z380059) and inserted into the well plate reader. The well-plate reader measured fluorescence output over the course of 11 h, and data points were graphed using Prism (n = 3 for each measurement).

Paper Discs Fabrication. Paper disc devices were fabricated according to previously published protocols.[15,22] Using AutoCAD, we designed paper disc devices with four separate loading zones: negative control (+beef/-biosensor), positive control (+putrescine/+biosensor), biosensor with no sample (-beef/+biosensor), and biosensor with sample (+beef/+biosensor). We constructed a device with four 5 mm disks separated by 9 mm center to center; this was done for two reasons: (1) to avoid cross contamination among samples and (2) to align with the wells in a 96 well-plate to enable fluorescence measurements.

Aluminum foil (Kingsford Extra Wide Aluminum, 25 μm), positional mounting adhesive (3M), and cold roll laminator (INTBUYING, Scarborough (ON), Canada) were purchased from Amazon. For the paper substrate, cellulose chromatography Whatman grade 1 (GE health care, 20 cm × 20 cm × 0.188 mm) was purchased from VWR. Whatman paper was affixed onto the mounting adhesive, gently peeled off, transferred onto an aluminum sheet, and trimmed to paper dimensions (measuring 20 cm × 20 cm). The foil-backed paper was fed through the cold-roll laminator to enable binding and to remove trapped air. The paper-device pattern was laser engraved using a 60 W CO_2 laser (Trotec Speedy, Trotec, Marchtrenk, Austria) with the following settings: 10% speed, 60% power, 1000 ppi, and 35 psi of compressed air.

Cell-Free Putrescine Biosensor System. Cell extract was prepared according to a modified protocol by Levine et al.[23] where *E. coli* BL21 DE3 star cells were transformed with repressor plasmid expressing the transcription factor PuuR. To make the cell extract for the cell-free biosensor, we followed protocols as described in Protocol S1. Cell-free protein synthesis (CFPS) solutions were prepared by mixing cell lysate (referred to as solution A), reaction buffer (solution B and solution C), reporter plasmid with P_{hyb} promoter, putrescine inducer, and water. Generally, three solutions were prepared to test the biosensor under cell-free conditions: solution A (15 mg/mL cell lysate as described in Protocol S1), solution B (1.2 mM ATP, 0.850 mM GTP, 0.850 mM UTP, 0.850 mM CTP, 31.50 μg/mL folinic acid, 170.60 μg/mL tRNA-*E. coli* MRE 600 (Roche, Sigma Millipore, 10109541001), 0.40 mM nicotinamide adenine dinucleotide (NAD), 0.27 mM coenzyme A (CoA), 4.00 mM oxalic acid, 1.50 mM spermidine, and 57.33 mM HEPES buffer), and solution C (2 mM $Mg(Glu)^2$, 10 mM $NH_4(Glu)$, 20 mM K(Glu), 2 mM each of the 20 amino acids, and 0.03 M phosphoenolpyruvate (PEP)). Prior to use,

https://doi.org/10.1021/acsabm.2c00824
ACS Appl. Bio Mater. 2022, 5, 5487−5496

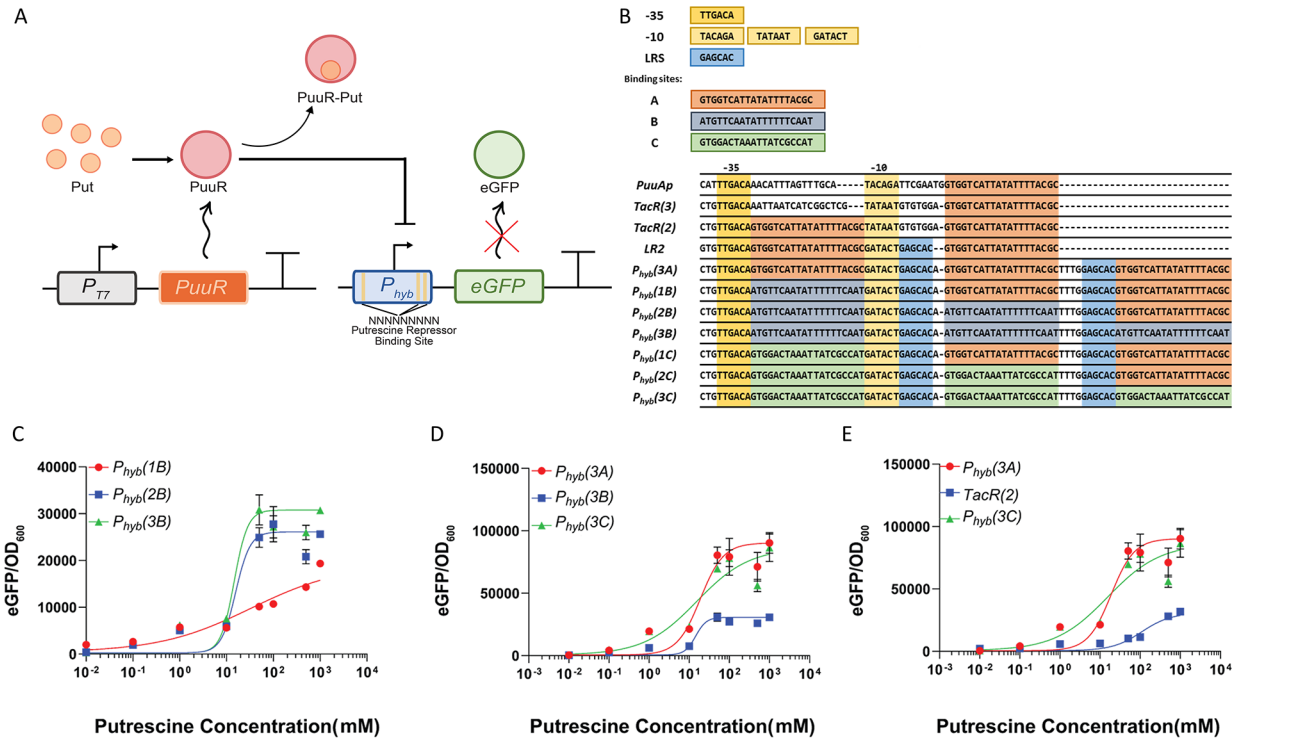

Figure 1. Synthetic putrescine biosensor. (A) Schematic of the transcription factor biosensor for the detection of putrescine. (B) DNA sequence of synthetic promoters PuuAp, TacR(3), TacR(2), and LR2 (Reproduced from Chen, X. F., Xia, X. X., Lee, S. Y., and Qian, Z. G. (2018) Engineering tunable biosensors for monitoring putrescine in *Escherichia coli*, *Biotechnol. Bioeng. 115*, 1014−1027[12] with permission) with *PuuR* binding regions, −35/−10 census sequences, and a LR-promoter spacer region. DNA sequences of hybrid synthetic promoters (P_{hyb}= P_{Tac}+ P_{LR}) for this study containing binding regions A (orange), B (blue), and/or C (green) were inserted either within or downstream of the −35 and −10 site. Dose−response semilog plots for whole cell sensors based on (C) different placements of the B binding site and (D) type of binding site measured at 16 h. (E) Two dose−response curves from this study [P_{hyb}(3A) and (3C)] were compared to the performance of TacR(2). All data points were represented as an average with error bars displaying standard error of the mean.

CFPS solutions were thawed on ice for 10−15 min and subsequently immobilized onto the paper device.

Immobilizing CFPS on the Paper Discs. Individual devices containing four discs were cut using a tabletop paper cutter (X-ACTO, Westerville (OH), United States), placed in a glass Petri dish, immersed in 4% BSA solution with 50 mM Tris buffer (pH = 7.5), and left to incubate for 1 h. Devices were transferred to a clean Petri dish and left to air-dry overnight, which was then ready for use. After drying, each reservoir was loaded with 5 μL of cell-free reaction (see Protocol S1 for cell-free reaction preparation). Two of the reservoirs were loaded with 5 μL of CFPS solutions without the reporter plasmid, and the other two reservoirs were loaded 5 μL of CFPS solutions with the reporter plasmid. Liquid nitrogen was poured over the paper devices and transferred to a lyophilization jar (Fast-Freeze Flask). Paper devices were lyophilized at 0.04 mbar at -50 °C for 12 h. For long-term storage, devices were stored in a box with calcium sulfate (Drierite) at room temperature.

Putrescine Biosensor Testing with Beef Samples. To study the bioaccumulation of putrescine in real beef samples, beef steak was purchased from a local grocery store. Beef was transported to the lab under ambient conditions from the local supermarket within 30 min. In the lab, beef was transferred to sterile containers and stored at -20 °C. Using a sterile razor blade, 5.0 g of beef was cut and weighed individually on separate and sterile boats. The meat was transferred to a 50 mL Falcon tubes, which were tightly sealed by wrapping the lids with Parafilm and immediately transferred to -20 °C. To determine the effect of temperature on meat quality, beef samples were subjected to different types of storage commonly used: fridge (4 °C), room temperature (20−25 °C), and frozen (-20 °C). The samples were left under these conditions for 4 days. On day 0 and on day 4, 1.0 g from the sample and 1.0 mL of phosphate buffer solution (PBS) were mixed and vortexed for 1 min to ensure uniform mixing between sample and PBS. Paper biosensors were rehydrated by adding 2.0 μL of the meat sample directly onto the paper disc of the device (which contained the CFPS solution). The device was incubated at room temperature (20−22 °C) until the entire device was saturated with sample for ∼30−60 s. The paper biosensor reservoirs were aligned with a center of the well, taped onto plate, and placed in the plate reader (CLARIOstar). The eGFP fluorescence was measured at λ_{ex} = 488 nm, λ_{em} = 507 nm, and gain = 1900 for the calibration curve (see Protocols S2 and S3). These devices were incubated at 30 °C for 1 to 6 h, and fluorescent measurements were pathway adjusted and well-scanned. The amount of putrescine in the meat samples was calculated from the calibration curve for promoter P_{hyb}(3A).

HPLC-MS Putrescine Quantification. Beef extracts were pelleted, and supernatants were filtered through a 0.2 μm sterile syringe filter. Filtered samples were diluted 1 in 100 in 15% acetonitrile (ACN) and were separated on a 1290 Infinity II liquid chromatography system (Agilent Technologies) using a Luna 5 μm NH2 100 Å, LC column 250 × 2 mm (Phenomenex) fitted with an autosampler that was cooled at 4 °C. Metabolites were separated using the following gradient of solvent A (0.1% formic acid in water) and solvent B (0.1% formic acid in 100% ACN):[24] 2% B to 10% B from 0 to 2 min (0.3 mL·min^{-1}), 10% B to 80% B from 2 to 5 min (0.3 mL·min^{-1}), 80% B to 3% B from 5 to 5.1 min (0.4 mL·min^{-1}), and held at 3% B from 5.1 to 6 min (0.4 mL·min^{-1}). After separation, the eluent was injected into a 6560 Ion Mobility Q-TOF (Agilent Technologies) using a 100 to 1100 m/z scanning range in positive mode. Data was processed using the Agilent Masshunter Quantitative Analysis software.

https://doi.org/10.1021/acsabm.2c00824
ACS Appl. Bio Mater. 2022, 5, 5487−5496

RESULTS AND DISCUSSION

Development of a Synthetic Putrescine Biosensor. We designed and constructed a putrescine sensor consisting of two genetic circuits: (i) the repressor and (ii) the sensing circuit (Figure 1A). The regulation of these circuits is coordinated through the T7 promoter regulated expression of the PuuR repressor, which binds to a synthetic putrescine-inducible promoter containing the operator *puuO* on the reporter plasmid. When there is a low level or absence of putrescine, the repressor, PuuR, will bind to the synthetic promoter and prevent eGFP production by blocking RNA polymerase from binding to *puuO*. In contrast, when putrescine is present, it will bind to PuuR, releasing it from *puuO* and allowing for RNA polymerase to bind to the promoter to enable eGFP expression.

There have been two reports[12,13] describing the development of synthetic promoters for detecting putrescine. In particular, in Chen et al., they modified the Tac (TacR) and the wild-type promoter (PuuAp) to monitor intracellular putrescine production. Tac is a hybrid of trp and lac promoters and is shown to be highly efficient in directing transcription, which can be attributed to the Tac promoter's tight regulation of expression.[25,26] Furthermore, they showed TacR to exhibit optimal performance and desirable activity, having the highest dynamic range providing resolution and accuracy when monitoring intracellular levels of putrescine.[12] Similarly, they also created a phage lambda promoter (LR2) that is also highly active *in vivo*, although it is recognized 15−30 times less *efficiently* by RNA polymerase.[27] Their work is an important step forward for detecting polyamines; however, their whole-cell biosensor was primarily optimized to monitor endogenous putrescine biosynthesis. Exogenously added putrescine showed changes in biosensing properties for different biosensor strains due to the putrescine metabolism in *E. coli* being easily altered by the extracellular putrescine. Given that putrescine metabolism is complicated and the requirements for a storage environment to maintain activity of the cell-based biosensors, these may prevent the deployment of the sensor to be used for meat quality control applications.[28] Therefore, to create a biosensor for amine detection in food samples, we report a new design of synthetic promoters that can be used for measuring exogenous putrescine from meat samples with faster response times and a higher dynamic range.

To engineer our library of synthetic promoters, we used two commonly used strategies: (1) modify the −35 and −10 consensus sequence and (2) add transcription factor binding regions at different locations within the operator.[9] As an initial design, we used the two highest dynamic range promoters, TacR(2) and LR2, from Chen et al.[12] and generated a hybrid promoter consisting of the "−10" site from the LR2 promoter and the "−35" site from TacR promoter because hybrid promoters are known to be highly efficient when directing transcription compared to nonhybrid promoters.[13,25] Next, we obtained sequences from *PuuA* and *PuuD* genes,[29,30] which are known PuuR binding regions, GTGGTCATTATATTTT-ACGC (we call "A"), ATGTTCAATATTTTTTCAAT (B), and GTGGACTAAATTATCGCCAT (C), and placed these binding regions within (W) and/or downstream (D) of the −35 and −10 sites to create different combinations of binding sites as it has been shown that mixing binding sites can lead to changes in the sensing and regulation.[29−31] Using these two strategies, we used 4 promoters from Chen et al.[12] as controls and created 7 hybrid promoters (Figure 1B).

Using our synthetic promoters, we measured the repression dynamics caused by PuuR. In the first step, the promoters were tested in the absence of IPTG (0 mM). We expect, without any repression, eGFP to be produced. As shown in Figure S1, regardless of the concentration of exogenously added putrescine, the plots confirm that fluorescence is always observed (i.e., no repression is occurring). In contrast, the sensors were interrogated with exogenously added IPTG at concentrations of 0.1 and 0.5 mM to induce PuuR expression. Generally, we observed a sigmoidal response curve with sharp increases in fluorescence at higher putrescine concentrations and low fluorescence output at low putrescine concentrations when the circuit was induced with 0.1 and 0.5 mM IPTG. There are two promoters that did not exhibit these biosensing characteristics: TacR(3) and P_{hyb}(1C). TacR(3) shows no repression behavior while P_{hyb}(1C) shows random fluorescence values for all tested putrescine concentrations. Given the poor characteristics, we eliminated both promoters from our quantification study (see below). Regardless, 6 out of the 7 designed promoters show regulation by induction with the 0.5 mM induction and provide dose-dependent Hill response properties indicating that PuuR is repressing the circuit when it is induced.

Interestingly, we observed differences in the output response when the promoters had different combinations of binding sites. When observing the output fluorescence levels at 0.5 mM induction for P_{hyb}(1B), P_{hyb}(2B), and P_{hyb}(3B), they show differences in their fluorescence output. Specifically, the output response for 2B and 3B showed increased sensitivity (depicted by the slope of the response curves) to putrescine and a lower response threshold (amount of putrescine for 50% output expression relative to baseline) (Figure 1C) compared to P_{hyb}(1B). Furthermore, we compared the output fluorescence containing the same type of binding site at all three regions. As shown in Figure 1D, binding sites A and C show similar dose−response curves but are different when compared to the curve given by B. The major difference is the maximum biosensor output, which is ∼2-fold larger for A and C compared to B. Finally, we compared the dose−response curves for hybrid 3A and 3C promoters with the Chen et al.[12] optimized whole-cell biosensor TacR(2). As shown in Figure 1E, we observe a higher sensitivity for our synthetic hybrid promoters compared to the TacR(2) promoter. We are unsure of what contributes to these differences observed with the different combinations of binding sites but hypothesize that changing the promoter operator site (number and type) changes the affinity of the transcription factor PuuR to the promoter site.[19,20,32] This is observed in other studies,[18,33,34] where one or two nucleotide changes in the operon can drastically change the overall dose−response dynamics. Indeed, more work is needed to understand these variations, but the performance is suitable for the detection of putrescine in beef samples (as described below).

Characterization of the Putrescine Biosensor. The safety and quality control of food, particularly meats, are usually monitored through the detection of biogenic amines.[34] Previous putrescine biosensors have two major drawbacks: the relatively limited dynamic range[12] and slow response to exogenous toxic concentrations of putrescine,[12,13] which are not suitable to detect our target concentrations of putrescine in meats. Our goal is to design a biosensor that can quickly and accurately detect putrescine concentrations at 39.76 mM and

https://doi.org/10.1021/acsabm.2c00824
ACS Appl. Bio Mater. 2022, 5, 5487−5496

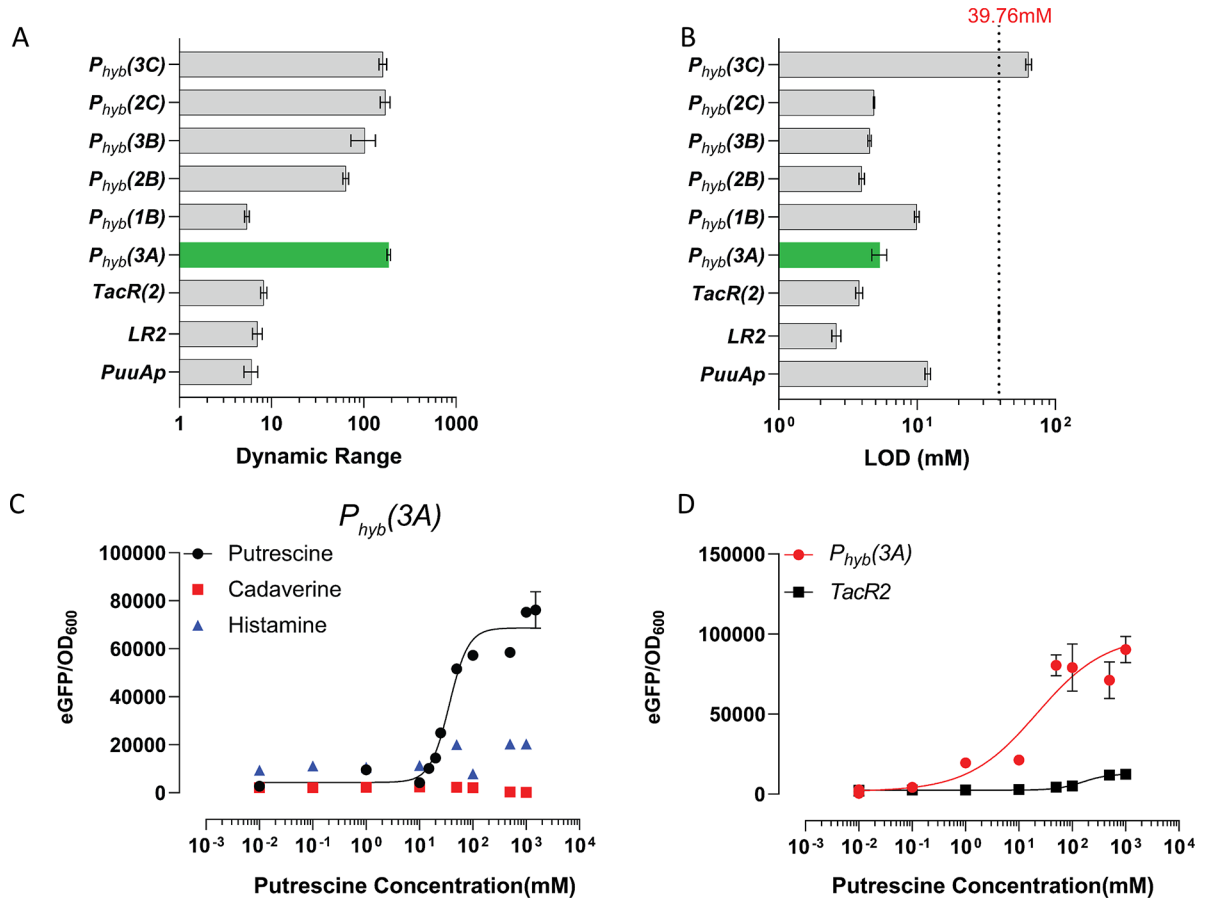

Figure 2. Quantification of dose−response parameters for PuuR response promoters. (A) Dynamic range shown for Chen et al.[12] promoters, PuuAp, LR2, and TacR(2), and six hybrid promoters developed in this study. The promoter with the highest dynamic range, P_{hyb}(3A), is highlighted in green. (B) Limit of detection (LOD) shown for all nine PuuR responsive promoters. The dotted line exhibits the target putrescine concentration (~39.76 mM). P_{hyb}(3A) has an LOD of 5.37 mM ± 0.66 and is highlighted in green. (C) Dose−response semilog curve displays the normalized fluorescence (over OD) for different concentrations of putrescine and in the presence of other BAs (cadaverine and histamine) for promoter P_{hyb}(3A). (D) Normalized fluorescence output showing the time response for whole cell biosensors containing TacR(2) (from Chen et al.[12]) or P_{hyb}(3A) (this study) promoters. All plots with error bars represent one standard error of the mean (N = three independent replicates). Values for promoters from Chen et al.[12] were reproduced from Chen, X. F., Xia, X. X., Lee, S. Y., and Qian, Z. G. (2018) Engineering tunable biosensors for monitoring putrescine in *Escherichia coli*, *Biotechnol. Bioeng. 115*, 1014−1027 with permission.

above the critical concentrations of putrescine in beef samples.[17,20] We quantified the dose−response parameters for our synthetic promoters: (1) dynamic range, which is the fold change in eGFP expression in the presence and absence of putrescine within the sample to provide the user more resolution into the level of spoilage, (2) limit of detection (LOD), which is the lowest concentration of putrescine in a sample the biosensor is capable of detecting, (3) specificity, which describes the biosensor's ability to sense putrescine in the presence of other BAs, and (4) time response, measuring how quickly our sensor can detect putrescine.

Dynamic Range. Dynamic range is quantified as the ratio of the highest measured output to the lowest measured output. A high dynamic range indicates an increased degree of confidence in the biosensors ability to measure a wide range of analyte concentrations.[35] As shown in Figure 2A, we evaluated 6 synthetic promoters (3 controls) and the dynamic range values are generally higher for the synthetic promoters that we designed compared to the Chen et al.[12] promoters: PuuAp, TacR(2), and LR2. For example, P_{hyb}(3A) showed a dynamic range of 186 ± 6.52 (p < 0.0001, N = 3 replicates), which is an ~33-fold increase compared to the dynamic range for PuuAp (5.54 ± 0.83). We also note the dynamic range for promoters with uniform binding sites are the highest. For example, P_{hyb}(1B), which contains a B binding site between −35 and −10 and two A binding sites downstream of the −10, shows a similar dynamic range as the control promoters of 3.36 ± 0.43. Comparing with P_{hyb}(3B), which only contains B binding sites (at the same locations), shows a dramatic 17-fold increase in dynamic range. In fact, P_{hyb}(3A), P_{hyb}(3B), and P_{hyb}(3C), all promoters with uniform binding sites (at the same locations), all show a similar dynamic range, ~178.3 ± 6.5, 156.1 ± 17.05, and 115.8 ± 25.05, respectively, and were observed to have the highest dynamic ranges of all synthetic promoters (with P_{hyb}(2C) as an exception).

Limit of Detection (LOD). Currently, there is no well-defined legal putrescine limit in North America despite the ability of putrescine to accumulate in very high concentrations for many food products.[36,37] However, one extensive study investigated the cytotoxic effects of putrescine when exposed to HT29 intestinal cells over a 24-h period. The results showed that the growth of HT29 cells were inhibited when putrescine reached a value of 39.8 mM or the half-maximal inhibitory concentration (IC_{50}).[38] We used this value as the defined limit

https://doi.org/10.1021/acsabm.2c00824
ACS Appl. Bio Mater. 2022, 5, 5487−5496

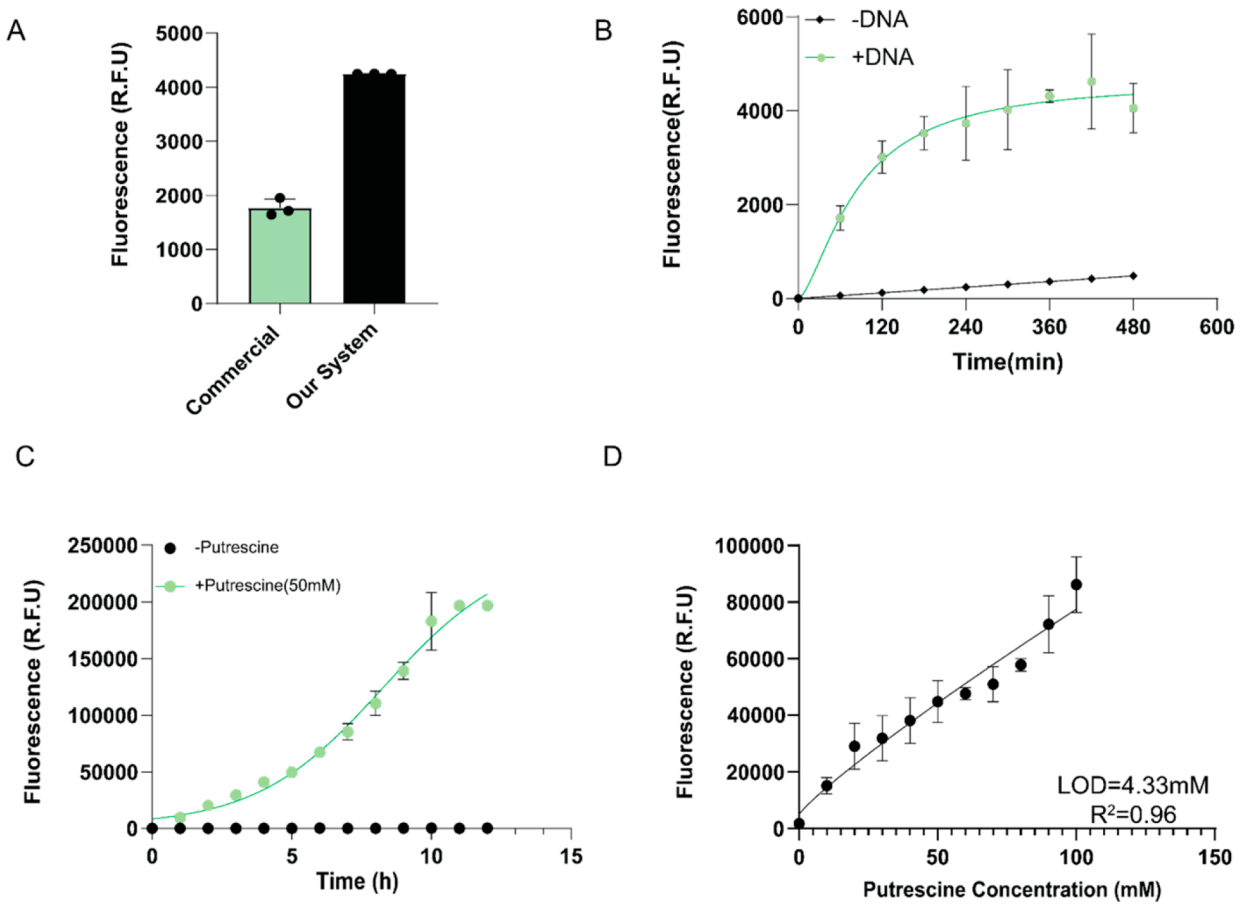

Figure 3. Optimization of our in-house cell-free system. (A) Comparison of the fluorescence values for our optimized cell-free reaction and a commercial lysate kit. (B) eGFP expression over time in a cell-free biosensor system measured by a well-plate reader. +DNA and −DNA contains the cell-free system with and without an eGFP plasmid driven by a constitutive promoter. (C) A spiked putrescine (50 mM) sample was added to the cell-free biosensor on paper and measured over time in a well plate reader. The absence of putrescine in the cell-free reaction was performed as a control. (D) A calibration curve for P_{hyb}(3A) was generated to quantify fluorescent outputs (from our cell-free lysate) to putrescine concentration. Putrescine was exogenously added with a concentration range of 10 to 100 mM to the cell-free reaction and incubated for 4 h at 30 °C. All data points are two biological replicates with error bars representing the standard error.

of putrescine, and as shown in Figure 2B, we found all promoters (except for P_{hyb}(3C)) to have an LOD lower than the target concentrations of putrescine. For P_{hyb}(3A) (which had the highest dynamic range), the LOD value was extrapolated from dose−response curves (Figure S2) and was found to be 5.37 mM ± 0.66, which is below the target 39.76 mM concentration.

Specificity. When constructing a biosensor for putrescine, there is a requirement to ensure strong and selective affinity between PuuR and the target analyte putrescine. Given that there are biogenic amines that are similar to putrescine in chemical structure, we wanted to assess their crosstalk. We selected two chemically similar and naturally occurring biogenic amines: cadaverine (1,5-diaminopentane) and histamine (2,4-imidazolyl-ethylamine). Promoter P_{hyb}(3A) was treated with putrescine and two other biogenic amines cadaverine and histamine. As shown in Figure 2C (for completion, see Figure S3 for other promoters), the dose−response curve showed minimal induction, where there is nonspecific binding between PuuR and cadaverine and histamine resulting in a dynamic range close to one. Significant lower percentages for histamine 2.5% ± 2.06 and cadaverine 2.84% ± 0.22 are observed for P_{hyb}(3A). These results are further supported by Chen et al.,[12] who showed that PuuR is evolved to be highly specific to putrescine and not toward other structurally similar biogenic amines (e.g., cadaverine). Given that P_{hyb}(3A) showed the optimal LOD, highest dynamic range, and minimal nonspecific binding, we determined this promoter to be best suited for our beef sample sensor.

Response Time. Response time is an important property to measure when characterizing biosensors, especially biosensors used for rapid diagnosis. Shorter or longer times to diagnosis can provide an indication of the time frame to obtain a result with shorter timeframes being more favorable for diagnostic devices. We measured the response time for our optimized promoter, P_{hyb}(3A). As shown in Figure 2D, the fluorescence levels for 50 mM putrescine-treated cells containing the P_{hyb}(3A) biosensor were higher after 1 h (compared to the starting level of fluorescence at 0 h). Measuring the fluorescence response over time, we observe stronger (and increasing) fluorescence levels and a more accurate response to the exogenous putrescine. In addition, we compared the response time of our biosensor to the optimal biosensor presented by Chen et al.[12] Interestingly, the responsiveness of our sensor was similar to that of TacR(2) up to 4 h. After 4 h, our sensor clearly shows a stronger response, which is expected given the sensitivity and dynamic range of our sensor is shown

https://doi.org/10.1021/acsabm.2c00824
ACS Appl. Bio Mater. 2022, 5, 5487−5496

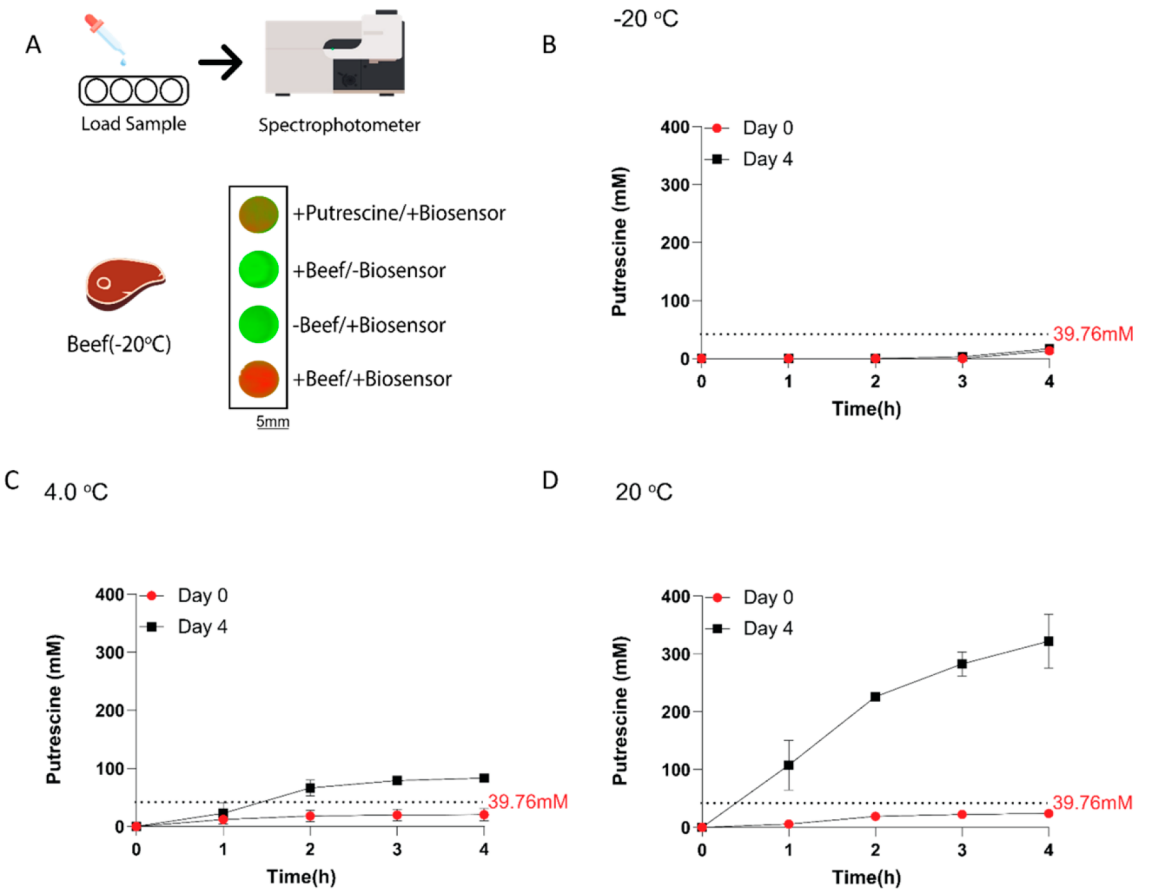

Figure 4. Assessment of putrescine in beef using our synthetic biosensor P_{hyb}(3A). (A) A well-scanned image of the fluorescence showing three controls (+put/+biosensor, +beef/−biosensor, −beef/+biosensor) and one beef sample (+beef/+biosensor) stored at -20 °C for 4 days. +Biosensor contains the CFPS solution with our putrescine biosensor system immobilized on the paper disc. Green and red indicates low and high fluorescence counts, respectively. (B−D) Kinetic plots showing the fluorescence of the putrescine content over 4 h when stored under three temperatures (B) −20 °C, (C) 4 °C, and (D) 20 °C. Putrescine content was measured each hour on the paper discs. The error bars represent one standard error for three biological independent replicates.

to be higher than those of TacR(2) (Figure 1E). In terms of diagnostics, the time-to-detection is lengthy (∼1 h) due to culturing, but modifying the circuit could potentially speed-up the output signal generation.

Cell-Free Biosensing. Cell-based biosensors are suitable for therapeutic applications[39] but are not suitable for field-based applications (e.g., spoiled meat detection) given the culture conditions and equipment that are needed to maintain the viability of the cells. To address this, we prepared our biosensor in a cell-free system.[14,40,41] One of the current limitations with cell-free systems is that they are costly. Many of these studies use commercial cell-free systems because of their strict quality control; however, it comes at a cost of ∼$3,383.00 USD (PURExpress), which translates to only 100 cell-free reactions.[42] To minimize cost, we developed an in-house crude cell-free system (motivated by Kwon and Jewett[43]), and from our calculations, we were able to minimize the cost from $33.83 USD per reaction to $1.52 USD/reaction using our cell-free system (Table S7, Figure S4). Although creating an in-house cell-free formulation can have significant cost benefits, there is the additional challenge of optimizing the system's parameters to enhance protein synthesis. To address this, we tested two main parameters that affect cell-free protein synthesis: ion concentration[22] (Figure S5A) and lysate composition[43] (Figure S5B). Magnesium is an essential cofactor for DNA replication,[44] transcription,[45] and neutralizing the charge on rRNA (rRNA).[46] Additionally, potassium ion concentrations need to be calibrated to stabilize functional mRNA, tRNA, and rRNA molecules.[47] From Figure S5A, we determined the optimal concentration for our cell-extract batch was 2 mM magnesium and 20 mM potassium for 30 μL of lysate. We also examined the proportion of lysate composition necessary for our biosensor to properly function and hypothesized that more lysate would result in higher eGFP transcription. However, the results indicated that, with the energy components, amino acids, and ions added to the solution, only 30 μL of cell-extract is required (Figure S5B), and this finding has been corroborated by other cell-free biosensors.[16,48,49] In addition, we compared the protein production between our cell-free formulation and a commercial kit (Expressway Mini Cell-Free Expression System, Invitrogen) (Figure 3A). Our formulation was shown to synthesize a higher protein yield in comparison to the commercial kit using our calibration curve. We produced 10.94 μg/mL ± 0.01 of eGFP protein in comparison to the commercial kit (Expressway Mini Cell-Free Expression System, Invitrogen), which produced 4.56 μg/mL ± 0.411 (a ∼2.4-fold increase in eGFP yield). We additionally tested our cell-free system by supplementing the cell-free reaction with a plasmid expressing eGFP under the control of a T7 promoter, and our

https://doi.org/10.1021/acsabm.2c00824
ACS Appl. Bio Mater. 2022, 5, 5487−5496

formulation was able to express eGFP over a span of 8 h (Figure 3B), which is suitable for our application below.

Testing the Biosensor with Real Beef Samples. To evaluate the potential use of our cell-free biosensor in a field setting, we designed a paper-disc device that can be used to store our cell-free components and as a diagnostic device to determine the putrescine content in meats. We were motivated by previous works that have used freeze-dried paper discs for disease-based diagnostics[15,50,51] and designed four discs on one device (Figure S6). To construct the devices, we took an approach described by Mahmud et al.[22] Following the workflow in Figure S7, cell-free reactions were added to the paper discs and lyophilized for 12 h prior to use with putrescine standards or meat solution samples. As an initial test, we validated our cell-free biosensor system on paper by adding putrescine (50 mM) to the cell lysate and evaluating eGFP expression under the control of P_{hyb}(3A) over the course of 12 h. After 1 h, we observed significant differences in the fluorescence (compared to the control), as shown in Figure 3C. Although our CFPS cocktail does not contain putrescine, we would expect that, with commercial CFPS cocktails[52] (which contain putrescine in the CFPS for efficient protein synthesis), our biosensor would produce minimal background fluorescence. However, the performance of our cell-free biosensor would continue to exhibit similar characteristics as our whole-cell biosensor. Next, to evaluate the performance of the cell-free biosensor, a series of putrescine calibrators ranging from 10 to 100 mM was prepared and evaluated in triplicates. As shown in Figure 3D, the fluorescence response for the optimized promoter, P_{hyb}(3A), was fitted to a linear regression, R^2 = 0.9, revealing a limit of detection of 4.33 mM ± 1.66 of putrescine, which is well below the defined limit for meat detection.

Prepared beef samples were stored at the different temperatures, and the samples stored at 4 and 20 °C had a foul smell after 3 days and 1 day of storage at their respective temperatures, suggesting they were not safe to eat. The beef sample stored at -20 °C did not have a foul smell after 4 days of storage. The extractant for each sample was loaded onto our paper devices followed by fluorescence measurements taken each hour for 4 h to measure their putrescine content (Figure 4A). Figure 4B−D presents our cell-free kinetic measurements for sensing putrescine in beef samples under different storage conditions. Each data point represents the putrescine concentration (converted using calibration curve), N = 3, between 1 and 4 h on either day 0 or 4 of storing the beef in common storage conditions such as in a fridge or freezer or at room temperature. As depicted in Figure 4B, after 4 days, the freezer storage led to the lowest putrescine production and that at room temperature showed the highest, exceeding the toxic threshold concentration. The beef extracts were also used for quantification by LC-MS. As expected, the values measured by our sensor are different from the values obtained by LC-MS (Figures S9 and S10). This is expected because there are other biogenic amines (tyramine, tryptamine, phenylethylamine) or compounds that can be converted to putrescine (glutamine/arginine → ornithine → putrescine) that are released during meat spoilage,[53,54] which could also be detected by our biosensor. Therefore, more work related to specificity or designing a multiplexed biosensor for detecting individual biogenic amines could be more indicative of correlating meat spoilage and biogenic amines.

As depicted in Figure 4B−D, the measurement was carried out after 4 h of incubation. We chose to arrest the measurement at 4 h because the putrescine levels surpassed the toxic levels after 2 and 1 h for beef stored at 4 and 20 °C for 4 days, respectively, indicating that the beef is not safe to consume. This is a notable result because our promoters show faster response times (compared to Chen et al.[12] promoters) when exposed to exogenous putrescine that is produced by real samples. We attribute the faster response times to having a cell-free system and an optimal promoter sequence for putrescine detection. Clearly, more work is required to improve the time to minutes for a rapid biosensor to indicate meat spoilage, and we propose the time might be lowered by using different lysate or cell media formulations,[12] an RNA-based sensor,[55] and nonfluorescence-based measurements.[56] However, the accuracy in determining spoilage at the higher temperature by measuring the putrescine concentration gives us confidence that we are able to use our hybrid-based promoter with a cell-free system on paper discs to detect putrescine in real meat samples.

CONCLUSION

In summary, we have successfully demonstrated the use of a cell-free paper-based biosensor for the detection of putrescine in beef under different storage conditions. Using a systematic engineering approach, we improved our biosensor performance by introducing different transcription factor-binding regions into promoters to make a specialized hybrid promoter. The new hybrid promoter is shown to have a high dynamic range and sensitivity, low background noise, LOD, and faster response time (~1 h). From quantification experiments, we observed an ~33-fold increase in dynamic range and a low detection limit of 5.34 mM. For field-testing purposes, we incorporated the cell-free biosensing with a paper-sensing device, making the device easy to use, portable, affordable, and biodegradable. Finally, we successfully demonstrated putrescine detection in real beef samples using the paper-based, cell-free biosensor. We propose that this new platform has great potential for the quantitative analysis of putrescine for other types of meats by including additional TFs that can sense other BAs that are relevant to the food industry.

ASSOCIATED CONTENT

Supporting Information

The Supporting Information is available free of charge at https://pubs.acs.org/doi/10.1021/acsabm.2c00824.

Supplementary protocols (preparation of cell lysate, quantification of reporter, construction of biosensor), tables (primer, DNA sequences for binding sites, PCR/Golden Gate conditions, cost comparison of materials for cell-free extract), and figures (repression dynamics, dose−response curves, specificity testing, cost-comparison of cell-free extract, paper-disc fabrication, HPLC-MS, and eGFP calibration curve) (PDF)

AUTHOR INFORMATION

Corresponding Author

Steve C. C. Shih − *Department of Biology, Concordia University, Montréal, Québec H4B 1R6, Canada; Centre for Applied Synthetic Biology, Concordia University, Montréal, Québec H4B 1R6, Canada; Department of Electrical and Computer Engineering, Concordia University, Montréal,*

https://doi.org/10.1021/acsabm.2c00824
ACS Appl. Bio Mater. 2022, 5, 5487−5496

Québec H3G 1M8, Canada; orcid.org/0000-0003-3540-0808; Phone: +1-(514) 848-2424; Email: steve.shih@concordia.ca

Authors

Alaa S. Selim − *Department of Biology, Concordia University, Montréal, Québec H4B 1R6, Canada; Centre for Applied Synthetic Biology, Concordia University, Montréal, Québec H4B 1R6, Canada*

James M. Perry − *Department of Biology, Concordia University, Montréal, Québec H4B 1R6, Canada; Centre for Applied Synthetic Biology, Concordia University, Montréal, Québec H4B 1R6, Canada*

Mohamed A. Nasr − *Department of Biology, Concordia University, Montréal, Québec H4B 1R6, Canada; Centre for Applied Synthetic Biology, Concordia University, Montréal, Québec H4B 1R6, Canada;* orcid.org/0000-0002-8921-6574

Jay M. Pimprikar − *Centre for Applied Synthetic Biology, Concordia University, Montréal, Québec H4B 1R6, Canada; Department of Electrical and Computer Engineering, Concordia University, Montréal, Québec H3G 1M8, Canada*

Complete contact information is available at: https://pubs.acs.org/10.1021/acsabm.2c00824

Author Contributions

All methodology, validation, formal analysis, investigation, review, editing, and visualization were done by A.S.S. Conceptualization, investigation, and reviewing and editing of manuscript were done by J.M.P. and M.A.N. Review, editing, and paper-device optimization and conceptualizing were done by J.M.P. Conceptualization, formal analysis, and review and editing of the manuscript were done by S.C.C.S.

Notes

The authors declare no competing financial interest.

■ ACKNOWLEDGMENTS

We would like to thank Dr. Micheal Pyne and Dr. Kealan Exley from the Martin Lab for extensive and fruitful discussions on protein expression and biosensing characterization. We would like to thank Dr. David Kwan, Dr. Ifthiha Mohideen, and Jama Ahmed for advice on protein expression and purification and access to the CLARIOstar. We would like to thank Marcos Di Falco for help with LC-MS analyses. We would also like to thank Dr. Smita Amarnath from the Genome Foundry for her help in experimental design and workflow. We thank the Natural Sciences and Engineering Research Council (NSERC), SynBioApps NSERC CREATE program, Fonds de Recherche Nature et technologies (FRQNT), and the Canadian Foundation of Innovation (CFI) for funding. S.C.C.S. thanks Concordia for a University Research Chair.

■ REFERENCES

(1) Wunderlichová, L.; Buňková, L.; Koutný, M.; Jančová, P.; Buňka, F. Formation, degradation, and detoxification of putrescine by foodborne bacteria: A review. *Comprehensive Review Food Science and Food Safety* **2014**, *13*, 1012−1030.

(2) del Rio, B.; Redruello, B.; Linares, D. M.; Ladero, V.; Ruas-Madiedo, P.; Fernandez, M.; Martin, M. C.; Alvarez, M. A. The biogenic amines putrescine and cadaverine show in vitro cytotoxicity at concentrations that can be found in foods. *Sci. Rep* **2019**, *9*, 120.

(3) Rauscher-Gabernig, E.; Gabernig, R.; Brueller, W.; Grossgut, R.; Bauer, F.; Paulsen, P. Dietary exposure assessment of putrescine and cadaverine and derivation of tolerable levels in selected foods consumed in Austria. *European Food and Technology* **2012**, *235*, 209−220.

(4) Bedia Erim, F. Recent Analytical Approaches to the Analysis of Biogenic Amines in Food Samples. *TrAC, Trends Anal. Chem. 2013* **2013**, *52*, 239−247.

(5) Jorgensen, L. V.; Huss, H. H.; Dalgaard, P. Significance of volatile compounds produced by spoilage bacteria in vacuum-packed cold-smoked salmon (Salmo salar) analyzed by GC-MS and multivariate regression. *J. Agric. Food Chem.* **2001**, *49*, 2376−2381.

(6) Boka, B.; Adanyi, N.; Szamos, J.; Virag, D.; Kiss, A. Putrescine biosensor based on putrescine oxidase from Kocuria rosea. *Enzyme Microb Technol.* **2012**, *51*, 258−262.

(7) Sudalaimani, S.; Esokkiya, A.; Hansda, S.; Suresh, C.; Tamilarasan, P.; Giribabu, K. ″Colorimetric Sensing of Putrescine and Cadaverine Using Ninhydrin as a Food Spoilage Detection Reagent.″. *Food Analytical Methods* **2020**, *13*, 629−636.

(8) Chen, S. Y.; Wei, W.; Yin, B. C.; Tong, Y.; Lu, J.; Ye, B. C. Development of a Highly Sensitive Whole-Cell Biosensor for Arsenite Detection through Engineered Promoter Modifications. *ACS Synth. Biol.* **2019**, *8*, 2295−2302.

(9) Zhang, F.; Carothers, J. M.; Keasling, J. D. Design of a dynamic sensor-regulator system for production of chemicals and fuels derived from fatty acids. *Nat. Biotechnol.* **2012**, *30*, 354−359.

(10) Wan, X.; Volpetti, F.; Petrova, E.; French, C.; Maerkl, S. J.; Wang, B. Cascaded amplifying circuits enable ultrasensitive cellular sensors for toxic metals. *Nat. Chem. Biol.* **2019**, *15*, 540−548.

(11) Mannan, A. A.; Liu, D.; Zhang, F.; Oyarzun, D. A. Fundamental Design Principles for Transcription-Factor-Based Metabolite Biosensors. *ACS Synth. Biol.* **2017**, *6*, 1851−1859.

(12) Chen, X. F.; Xia, X. X.; Lee, S. Y.; Qian, Z. G. Engineering tunable biosensors for monitoring putrescine in *Escherichia coli*. *Biotechnol. Bioeng.* **2018**, *115*, 1014−1027.

(13) Zhao, N.; Song, J.; Zhang, H.; Lin, Y.; Han, S.; Huang, Y.; Zheng, S. Development of a Transcription Factor-Based Diamine Biosensor in Corynebacterium glutamicum. *ACS Synth. Biol.* **2021**, *10*, 3074−3083.

(14) Grawe, A.; Dreyer, A.; Vornholt, T.; Barteczko, U.; Buchholz, L.; Drews, G.; Ho, U. L.; Jackowski, M. E.; Kracht, M.; Luders, J.; Bleckwehl, T.; Rositzka, L.; Ruwe, M.; Wittchen, M.; Lutter, P.; Muller, K.; Kalinowski, J. A paper-based, cell-free biosensor system for the detection of heavy metals and date rape drugs. *PLoS One* **2019**, *14*, No. e0210940.

(15) Thavarajah, W.; Silverman, A. D.; Verosloff, M. S.; Kelley-Loughnane, N.; Jewett, M. C.; Lucks, J. B. Point-of-Use Detection of Environmental Fluoride via a Cell-Free Riboswitch-Based Biosensor. *ACS Synth. Biol.* **2020**, *9*, 10−18.

(16) Voyvodic, P. L.; Pandi, A.; Koch, M.; Conejero, I.; Valjent, E.; Courtet, P.; Renard, E.; Faulon, J. L.; Bonnet, J. Plug-and-play metabolic transducers expand the chemical detection space of cell-free biosensors. *Nat. Commun.* **2019**, *10*, 1−8.

(17) Chen, X.; Gao, C.; Guo, L.; Hu, G.; Luo, Q.; Liu, J.; Liu, L. DCEO Biotechnology: Tools To Design, Construct, Evaluate, Optimize the Metabolic Pathway for Biosynthesis of Chemicals. *Chem. Rev.* **2018**, *118*, 4−72.

(18) Mannan, A. A.; Liu, D.; Zhang, F.; Oyarzun, D. A. Fundamental Design Principles for Transcription-Factor-Based Metabolite Biosensors. *ACS Synth. Biol.* **2017**, *6*, 1851−1859.

(19) De Paepe, B.; Peters, G.; Coussement, P.; Maertens, J.; De Mey, M. Tailor-made transcriptional biosensors for optimizing microbial cell factories. *J. Ind. Microbiol Biotechnol* **2017**, *44*, 623−645.

(20) Ding, N.; Zhou, S.; Deng, Y. Transcription-Factor-based Biosensor Engineering for Applications in Synthetic Biology. *ACS Synth. Biol.* **2021**, *10*, 911−922.

(21) Armbruster, D. A.; Pry, T. Limit of blank, limit of detection and limit of quantitation. *Clin Biochem Rev.* **2008**, *1*, S49−S52.

(22) Mahmud, M. A.; Blondeel, E. J.; Kaddoura, M.; MacDonald, B. D. Creating compact and microscale features in paper-based devices by laser cutting. *Analyst* **2016**, *141*, 6449−6454.

(23) Levine, M. Z.; Gregorio, N. E.; Jewett, M. C.; Watts, K. R.; Oza, J. P. Escherichia coli-Based Cell-Free Protein Synthesis: Protocols for a robust, flexible, accessible platform technology. *J. Vis Exp* **2019**, No. e58882.
(24) Ducros, V.; Ruffieux, D.; Belva-Besnet, H.; de Fraipont, F.; Berger, F.; Favier, A. Determination of dansylated polyamines in red blood cells by liquid chromatography-tandem mass spectrometry. *Anal. Biochem.* **2009**, *390*, 46−51.
(25) Amann, E.; Ochs, B.; Abel, K. J. Tightly regulated tac promoter vectors useful for the expression of unfused and fused proteins in Escherichia coli. *Gene* **1988**, *69*, 301−315.
(26) de Boer, H. A.; Comstock, L. J.; Vasser, M. The tac promoter: a functional hybrid derived from the trp and lac promoters. *Proc. Natl. Acad. Sci. U. S. A.* **1983**, *80*, 21−25.
(27) Knaus, R.; Bujard, H. PL of coliphage lambda: an alternative solution for an efficient promoter. *EMBO J.* **1988**, *7*, 2919−2923.
(28) Park, Y.; Kim, S. M.; Lee, J. Y.; Jang, W. Application of biosensors in smart packaging. *Molecular & Cellular Toxicology* **2015**, *11*, 277−285.
(29) Nemoto, N.; Kurihara, S.; Kitahara, Y.; Asada, K.; Kato, K.; Suzuki, H. Mechanism for regulation of the putrescine utilization pathway by the transcription factor PuuR in Escherichia coli K-12. *J. Bacteriol.* **2012**, *194*, 3437−3447.
(30) Kurihara, S.; Tsuboi, Y.; Oda, S.; Kim, H. G.; Kumagai, H.; Suzuki, H. The putrescine Importer PuuP of Escherichia coli K-12. *J. Bacteriol.* **2009**, *191*, 2776−2782.
(31) Collado-Vides, J.; Magasanik, B.; Gralla, J. D. Control site location and transcriptional regulation in Escherichia coli. *Microbiol Rev.* **1991**, *55*, 371−394.
(32) Crocker, J.; Noon, E. P.; Stern, D. L. The Soft Touch: Low-Affinity Transcription Factor Binding Sites in Development and Evolution. *Curr. Top Dev Biol.* **2016**, *117*, 455−469.
(33) David, A. A.; Terry, P. Limit of Blank, Limit of Detection and Limit of Quantitation. *Clin. Biochem. Rev.* **2008**, *29*, S49−S52.
(34) John, D. C.; Birgit, N.; Herbert, B.; Olivier, A.; Sava, B.; John, G.; Tine, H.; Arie, H.; James, H.; Günter, K.; Kostas, K.; James, M.; Christine, M.; Christophe, N.; Luisa, P. Scientific Opinion on risk based control of biogenic amine formation in fermented foods. *European Food Safety Authority (EFSA)* **2011**, *9*, 2393.
(35) Berepiki, A.; Kent, R.; Machado, L. F. M.; Dixon, N. Development of High-Performance Whole Cell Biosensors Aided by Statistical Modeling. *ACS Synth. Biol.* **2020**, *9*, 576−589.
(36) Atiya Ali, M.; Poortvliet, E.; Stromberg, R.; Yngve, A. Polyamines in foods: development of a food database. *Food & Nutrition Research* **2011**, *55*, 5572.
(37) Rauscher-Gabernig, E.; Gabernig, R.; Brueller, W.; Grossgut, R.; Bauer, F.; Paulsen, P. Dietary exposure assessment of putrescine and cadaverine and derivation of tolerable levels in selected foods consumed in Austria. *European Food and Technology* **2012**, *235*, 209−220.
(38) del Rio, B.; Redruello, B.; Linares, D. M.; Ladero, V.; Ruas-Madiedo, P.; Fernandez, M.; Martin, M. C.; Alvarez, M. A. biogenic amines putrescine and cadaverine show in vitro cytotoxicity at concentrations that can be found in foods. *Sci. Rep.* **2019**, *9*, 120.
(39) Bloemberg, D.; Nguyen, T.; MacLean, S.; Zafer, A.; Gadoury, C.; Gurnani, K.; Chattopadhyay, A.; Ash, J.; Lippens, J.; Harcus, D.; Page, M.; Fortin, A.; Pon, R. A.; Gilbert, R.; Marcil, A.; Weeratna, R. D.; McComb, S. A High-Throughput Method for Characterizing Novel Chimeric Antigen Receptors in Jurkat Cells. *Mol. Ther Methods Clin Dev* **2020**, *16*, 238−254.
(40) Chen, S.-Y.; Wei, W.; Yin, B.-C.; Tong, Y.; Lu, J.; Ye, B.-C. Development of a Highly Sensitive Whole-Cell Biosensor for Arsenite Detection through Engineered Promoter Modifications. *ACS Synth. Biol.* **2019**, *8*, 2295−2302.
(41) Zhang, L.; Guo, W.; Lu, Y. Advances in Cell-Free Biosensors: Principle, Mechanism, and Applications. *Biotechnology Journal* **2020**, *15*, 2000187.
(42) Lavickova, B.; Maerkl, S. J. A simple, robust, and low-cost method to produce the PURE cell - free system. *ACS Synth. Biol.* **2019**, *8*, 455−462.
(43) Kwon, Y. C.; Jewett, M. C. High-throughput preparation methods of crude extract for robust cell-free protein synthesis. *Sci. Rep* **2015**, *5*, 8663.
(44) Hartwig, A. Role of magnesium in genomic stability. *Mutation Research/Fundamental and Molecular Mechanisms of Mutagenesis* **2001**, *475*, 113−121.
(45) Misra, V. K.; Draper, D. E. The linkage between magnesium binding and RNA folding. *J. Mol. Biol.* **2002**, *317*, 507−521.
(46) Pontes, M. H.; Yeom, J.; Groisman, E. A. Reducing Ribosome Biosynthesis Promotes Translation during Low Mg(2+) Stress. *Mol. Cell* **2016**, *64*, 480−492.
(47) Rozov, A.; Khusainov, I.; El Omari, K.; Duman, R.; Mykhaylyk, V.; Yusupov, M.; Westhof, E.; Wagner, A.; Yusupova, G. Importance of potassium ions for ribosome structure and function revealed by long-wavelength X-ray diffraction. *Nat. Commun.* **2019**, *10*, 2519.
(48) Jung, J. K.; Alam, K. K.; Verosloff, M. S.; Capdevila, D. A.; Desmau, M.; Clauer, P. R.; Lee, J. W.; Nguyen, P. Q.; Pasten, P. A.; Matiasek, S. J.; Gaillard, J. F.; Giedroc, D. P.; Collins, J. J.; Lucks, J. B. Cell-free biosensors for rapid detection of water contaminants. *Nat. Biotechnol.* **2020**, *38*, 1451−1459.
(49) Pandi, A.; Grigoras, I.; Borkowski, O.; Faulon, J. L. Optimizing Cell-Free Biosensors to Monitor Enzymatic Production. *ACS Synth. Biol.* **2019**, *8*, 1952−1957.
(50) Pardee, K.; Green, A. A.; Ferrante, T.; Cameron, D. E.; DaleyKeyser, A.; Yin, P.; Collins, J. J. Paper-based synthetic gene networks. *Cell* **2014**, *159*, 940−954.
(51) Didovyk, A.; Tonooka, T.; Tsimring, L.; Hasty, J. Rapid and Scalable Preparation of Bacterial Lysates for Cell-Free Gene Expression. *ACS Synth. Biol.* **2017**, *6*, 2198−2208.
(52) Miguez, A. M.; McNerney, M. P.; Styczynski, M. P. Metabolic Profiling of Escherichia coli-based Cell-Free Expression Systems for Process Optimization. *Ind. Eng. Chem. Res.* **2019**, *58*, 22472−22482.
(53) Vinci, G.; Antonelli, M. L. Biogenic amines: quality index of freshness in red and white meat. *Food Control* **2002**, *13*, 519−524.
(54) Wunderlichová, L.; Buňková, L.; Koutný, M.; Jančová, P.; Buňka, F. Formation, degradation, and detoxification of putrescine by foodborne bacteria: A review. *Comprehensive Review Food Science and Food Safety* **2014**, *13*, 1012−1030.
(55) Karlikow, M.; da Silva, S. J. R.; Guo, Y.; Cicek, S.; Krokovsky, L.; Homme, P.; Xiong, Y.; Xu, T.; Calderon-Pelaez, M.-A.; Camacho-Ortega, S.; Ma, D.; de Magalhaes, J. J. F.; Souza, B. N. R. F.; de Albuquerque Cabral, D. G.; Jaenes, K.; Sutyrina, P.; Ferrante, T.; Benitez, A. D.; Nipaz, V.; Ponce, P.; Rackus, D. G.; Collins, J. J.; Paiva, M.; Castellanos, J. E.; Cevallos, V.; Green, A. A.; Ayres, C.; Pena, L.; Pardee, K. Field validation of the performance of paper-based tests for the detection of the Zika and chikungunya viruses in serum samples. *Nat. Biomed Eng.* **2022**, *6*, 246−256.
(56) Sadat Mousavi, P.; Smith, S. J.; Chen, J. B.; Karlikow, M.; Tinafar, A.; Robinson, C.; Liu, W.; Ma, D.; Green, A. A.; Kelley, S. O.; Pardee, K. A multiplexed, electrochemical interface for gene-circuit-based sensors. *Nat. Chem.* **2020**, *12*, 48−55.

https://doi.org/10.1021/acsabm.2c00824
ACS Appl. Bio Mater. 2022, 5, 5487−5496